

Anisotropic fracture toughness of Poorman Schist rocks from EGS Collab Experiment 1 Site

Ruplinger, C., *O'Connell, R., Sone, H., Trzeciak, M. and Wang, H.

University of Wisconsin-Madison, Madison, Wisconsin, USA

* Now at Colorado School of Mines, Golden, Colorado, USA

Copyright 2020 ARMA, American Rock Mechanics Association

This paper was prepared for presentation at the 54th US Rock Mechanics/Geomechanics Symposium held in Golden, Colorado, USA, 28 June-1 July 2020. This paper was selected for presentation at the symposium by an ARMA Technical Program Committee based on a technical and critical review of the paper by a minimum of two technical reviewers. The material, as presented, does not necessarily reflect any position of ARMA, its officers, or members. Electronic reproduction, distribution, or storage of any part of this paper for commercial purposes without the written consent of ARMA is prohibited. Permission to reproduce in print is restricted to an abstract of not more than 200 words; illustrations may not be copied. The abstract must contain conspicuous acknowledgement of where and by whom the paper was presented.

ABSTRACT: We investigate the mode 1 fracture toughness and its anisotropy of Poorman Schist rocks recovered from the Enhanced Geothermal Systems Collaboration (EGS Collab) Experiment 1 site. The EGS Collab team is conducting a series of intermediate (10-20m) scale stimulation and inter-well flow tests with comprehensive instrumentation and characterization at the Sanford Underground Research Facility to validate existing theories and description of hydraulic fractures propagation and associated fluid flow. An important parameter to constrain is how the fracture toughness varies depending on the orientation of the fracture and the direction of fracture propagation, which may have controls on hydraulic fracture propagation. Fracture toughness relative to foliation orientation was determined through the utilization of Cracked Chevron Notched Brazilian Disk (CCNBD) samples in three different orientations (Divider, Arrester, and Foliation Splitting/Short Transverse). Each sample group contains at least three 25.4 mm diameter and 12.7 mm thick CCNBD samples, one of each sample type. Arrester and Foliation Splitting samples were obtained from the same sub-core while Divider samples were obtained from a separate sub-core obtained in close proximity. We found fracture toughness to be weakest in the Foliation Splitting orientation and strongest in the Divider orientation, similar to findings from anisotropic fracture toughness measured in shale rocks. Our findings on the influence of foliation orientation on fracture toughness are presented here.

1. INTRODUCTION

The Enhanced Geothermal Systems (EGS) Collaboration project's goal is to improve the feasibility of large-scale EGS resources by better understanding the relation between permeability enhancement and fractures in crystalline rock. To better understand fracture stimulation methods, fracture geometries, and processes controlling heat transfer between crystalline rock and stimulated fractures, a group of test beds (10-20 m) were established for stimulation and testing (Kneafsey et al., 2018).

Experiment 1 of the EGS Collaboration project takes place in the Poorman schist at the Sanford Underground Research Facility (SURF) in Lead, South Dakota. The Poorman schist is a foliated unit consisting of calcite, muscovite, dolomite, biotite, quartz, and chlorite. Foliations can be observed in planar and tightly folded orientations. These folds vary in size from centimeters to meters.

To relate Mode I fracture toughness to foliation orientation, we utilized Cracked Chevron Notched Brazilian Disc (CCNBD) samples in three sample orientations; the Divider, Arrester, and Foliation Splitting orientations as seen in Figure 1. Note that, prior to this study, the orientation we refer to as foliation splitting has also been referred to as short transverse (Chong et al.,

1987). Previous studies on other foliated rocks have shown the Divider orientation to be slightly stronger than the arrester orientation with the foliation splitting orientation being the weakest (Chandler et al., 2016; Schmidt and Huddle, 1977). We investigate the influence of foliation orientation on the fracture toughness of the Poorman Schist at the EGS Collaboration Experiment 1 site.

The CCNBD geometry was selected to measure Mode I fracture toughness for reasons identified by Fowell and Xu (1994). CCNBD samples offer simplified sample preparation and testing setups, high failure loads, and a range of valid sample dimensions. In addition, CCNBD samples allow for the crack orientation to be adjusted with respect to the rock texture, allowing for fracture toughness to be determined as a function of fracture orientation.

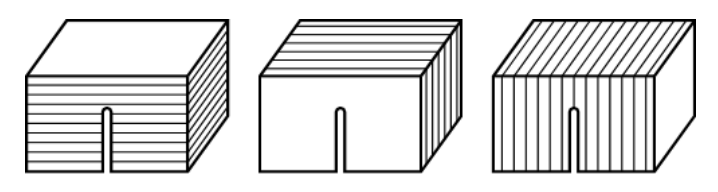


Fig. 1. The principal notch orientations with respect to foliation planes (left to right: arrester, divider, and foliation splitting/short transverse). Figure reproduced from Chong et al., 1987.

2. SAMPLE SELECTION AND PREPERATION

Representative cores of the Poorman Schist were subcored to 38.1 mm (1.5 inch) diameter cylinders with varying lengths due to changing foliation orientation. Sub-cores were cored in one of two orientations, as shown in Figure 2. These cores were then sliced into 12.7 mm (0.5 inch) thick discs with a precision rock saw. The Chevron notches were cut following the method outlined by Chang et al. (2002). A custom setup was designed to control notch depth. This setup used a 25.4 mm (1 inch) diamond blade attachment for a rotary hand tool with the rotary hand tool secured such that the blade was normal to the work surface. Two posts with depth controls were placed in the same plane as the diamond blade. A sample holder was designed to slide on the posts such that the diamond blade was aligned with the desired notch orientation.

Using the custom setup, a Brazilian disc sample was lowered onto the diamond blade to a set depth determined by sample thickness and diameter. The sample and sample holder were then raised, removed from the posts, and flipped 180 degrees. A second cut was made to the same depth as the first cut. All dimensions were determined from the range of valid geometric dimensions provided in the ISRM suggested methods (Fowell, 1995) as shown in Figure 3.

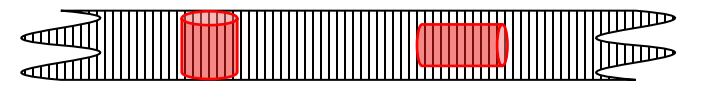


Fig. 2. Orientations of sub-cores with respect to the overall core and foliations. The left sub-core was used for foliation splitting and arrest samples while the right was used for divider samples.

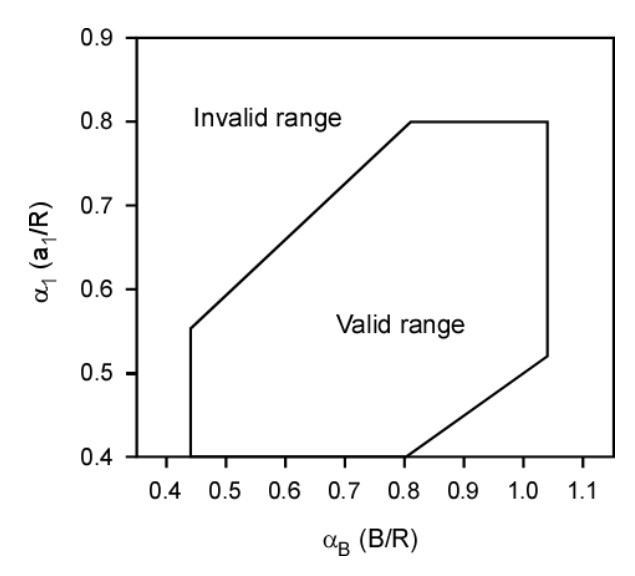


Fig. 3. The geometric dimensions established in the ISRM suggested methods with variables of B (thickness), R (radius), and a_1 (chevron notch length at disk surface). α_B and α_1 are ratios of these geometric dimensions. Figure reproduced from Fowell, 1995.

Sample groups were cored in close proximity in order to reduce the effects of heterogeneity. The goal was to produce three samples, one of each orientation, with similar mineral compositions and foliation characteristics. A total of 19 notched Brazilian disk samples were prepared representing 5 sample groups.

After fracture toughness testing, a representative sample from each sample group was made into a thin section for inspection of fabric and mineralogy.

3. LABORATORY METHODS

All samples were tested for fracture toughness with a servo controlled triaxial testing system with no confining pressure and at room temperature. A custom-made jaw fixture, as seen in Figure 4, following specifications described in the ISRM suggested method was used to hold the samples and apply a diametric compressional load. Two linear variable differential transformers (LVDT) were used to record vertical displacement of the upper jaw relative to the lower jaw, while a strain gauge-based displacement transducer was used to record horizontal expansion of the samples.

Each sample was tested with a two-phase test procedure. In the first phase, the piston advanced until a load of 0.1 kN was reached by the load cell. This was done to ensure that phase two started in contact with the sample. In phase two, the sample was loaded under displacement control while the diametrical load, vertical displacement and load-normal expansion was recorded. Each test was run until the sample experienced structural failure. After testing, an optical microscope was used to inspect fabric and mineralogy characteristics of the Poorman Schist samples.



Fig. 4. The test fixture with a post-test sample.

4. RESULTS

4.1. Experimental Observations

A plot of the load vs. time for Group 1 samples are shown in Figure 5. The diametrical load at which structural failure occurs, which is used for fracture toughness calculations, is marked with a black X. Structural failure for all samples was experienced at 8-30 seconds into the test. All sample IDs and the corresponding maximum diametrical loads are shown in Table 1.

Figure 6 shows a plot of the load vs. average LVDT displacement for Group 1 samples. Again, the diametrical load at structural failure is marked with a black X. All samples showed load-displacement behavior that follows the three stages, identified in Guo (1993), of (1) elastic behavior from test initiation to maximum load, (2) unstable crack propagation until a local minimum load is reached, and (3) increasing load allowing for further cracks to propagate, although only stages 1 and 2 are shown in the Figure 6. Samples failed after LVDT displacements between 0.05 and 0.35 mm. Note that the slope of the divider and foliation splitting samples are steeper than the arrester samples. This is consistent with the transversely isotropic nature of the schist rocks where the elastic modulus is higher when loaded parallel to the foliations.

Table 1. Sample orientation, maximum frame load, and fracture toughness.

Group		Sample	Maximum	Fracture
number and		Orientation	Diametrical	Toughness
Sample ID			Load (kN)	(MPa m ^{1/2})
1	1.1	Divider	5.80	2.05
	1.2	Divider	5.41	1.85
	2.1	Fol. Splitting	3.36	1.13
	2.2	Arrester	3.86	1.41
2	3.1	Divider	5.93	2.05
	3.2	Divider	5.29	1.84
	4.1	Fol. Splitting	1.36	0.48
	4.3	Arrester	0.91	0.30
3	5.1	Divider	3.03	1.00
	7.1	Arrester	4.84	1.68
4	9.1	Fol. Splitting	2.50	0.94
	9.2	Arrester	4.24	1.49
	10.1	Divider	1.61	0.55
	10.2	Divider	4.24	1.49
	10.3	Divider	4.83	1.76
5	11.1	Fol. Splitting	1.52	0.54
	11.3	Arrester	3.92	1.36
	12.1	Divider	6.41	2.23
	12.2	Divider	5.45	1.98

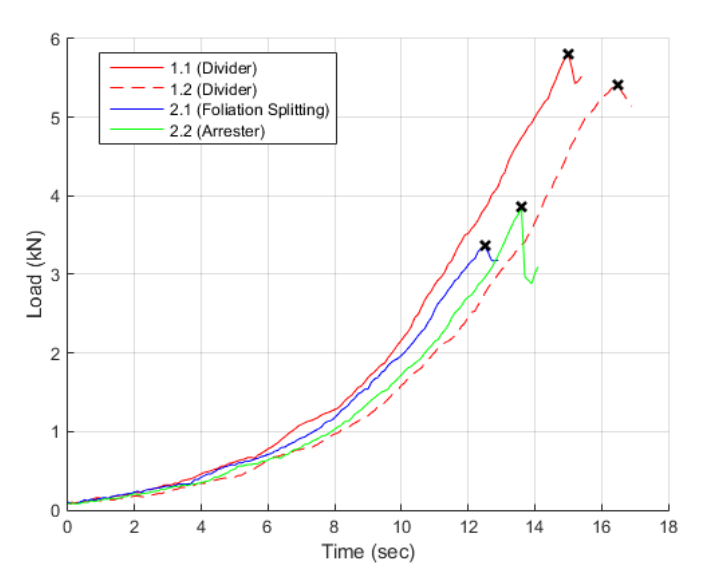


Fig. 5. Load vs. time of Group 1 samples.

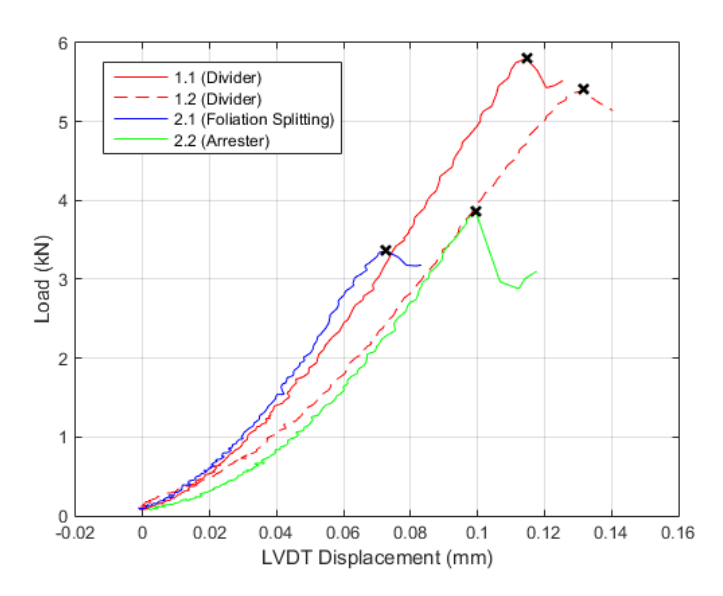


Fig. 6. Load vs. LVDT displacement of Group 1 samples.

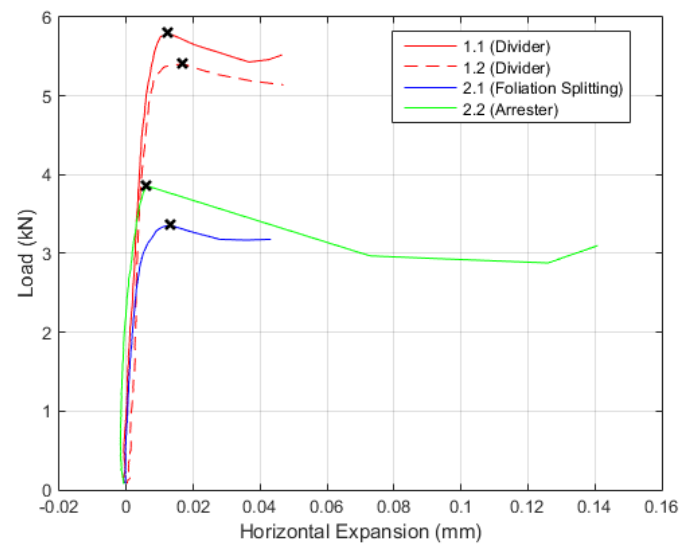


Fig. 7. Load vs. horizontal expansion of Group 1 samples.

The load vs. horizontal expansion for Group 1 samples is shown in Figure 7. All samples experienced structural failure with horizontal expansion between 0.005 and 0.06 mm. All but one sample (10.1) followed a similar trend of increasing horizontal expansion with increasing load until structural failure. After structural failure, load dissipated while LDT displacement continued to increase.

4.2. Fracture Toughness Results

Fowell (1995) suggests an equation for calculating the fracture toughness of rocks from CCNBD samples:

$$K_{IC} = \frac{P_{max}}{B*\sqrt{D}} * Y_{min}^*$$
 (1)

where K_{IC} is fracture toughness, P_{max} is maximum diametrical load, B is sample thickness, D is sample diameter, and Y^*_{min} is the critical dimensionless stress intensity factor for the specimen dependent on the specimen geometry. Y^*_{min} is calculated using the following formula:

$$Y_{min}^* = u * e^{v*\alpha_1} \tag{2}$$

where u and v are geometric constants determined from α_0 , α_1 and α_B , which are defined as:

$$\alpha_0 = \frac{a_0}{R} \tag{3}$$

$$\alpha_1 = \frac{a_1}{R} \tag{4}$$

$$\alpha_B = \frac{B}{R} \tag{5}$$

 a_0 is the initial chevron notch crack length, a_1 is the final chevron notch crack length, and R is disk radius. From these geometric dimensions, the constants u and v are linearly interpolated from values in Table 2 of Fowell, 1995, the ISRM suggested method.

Using Eq. (2)-(5), the dimensionless stress intensity factor, Y^*_{min} , was calculated for each sample based on geometric measurements taken before testing for fracture toughness. After calculating Y^*_{min} , the fracture toughness was calculated using Eq. (1). The calculated fracture toughness values are listed in Table 1 and also shown in Figure 8.

5. DISCUSSION

The fracture toughness testing of the three different orientations suggest that fracture toughness is significantly weaker in the foliation splitting orientation than the other orientations. In the foliation splitting orientation, the fractures propagate in the same plane as the foliations, which are found to be the weak planes in these rock types (Condon et al., 2019), thus likely leading to low fracture toughness.

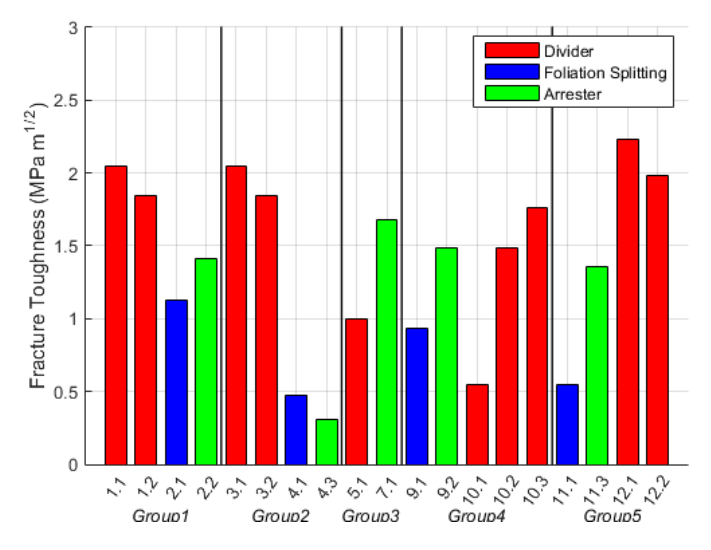


Fig. 8. Fracture toughness values determined from the experiments.

In the divider orientation, the fracture propagates through all foliation planes simultaneously. The simultaneous fracturing allows for weaker and stronger planes to act as a single unit, producing a sample harder to fracture. In the arrester sample, the fracture propagates through each foliation plane individually, potentially allowing for variability in fracture toughness as the fracture propagate through different foliation layers. Whether the divider or arrester orientation should appear stronger or weaker requires careful discussion, but our results suggest that the divider orientation is stronger. This is indeed consistent with results from Schmidt and Huddle (1977) and Chandler (2016) where fracture toughness was found to be stronger in the divider orientation than arrester orientation for Anvil Point oil shale and Mancos shale samples, respectively (Table 2).

Table 2. Fracture toughness of Mancos shale samples reported in Chandler et al. (2016) and Anvil Point oil shales in Schmidt and Huddle (1977). Oil shales B and D have nominal kerogen content of 20 and 40 gal/ton, respectively

Sample	Orientation	Fracture Toughness (MPa m ^{1/2})	
	Divider	0.72	
Mancos Shale	Arrester	0.62	
211412	Short Transverse	0.21 - 0.52	
Anvil	Divider	1.02 - 1.13	
Point Oil Shale	Arrester	0.92 - 0.95	
Block B	Short Transverse	0.75	
Anvil	Divider	0.64 - 0.67	
Point Oil Shale	Arrester	0.60 - 0.61	
Block D	Short Transverse	0.32 - 0.41	

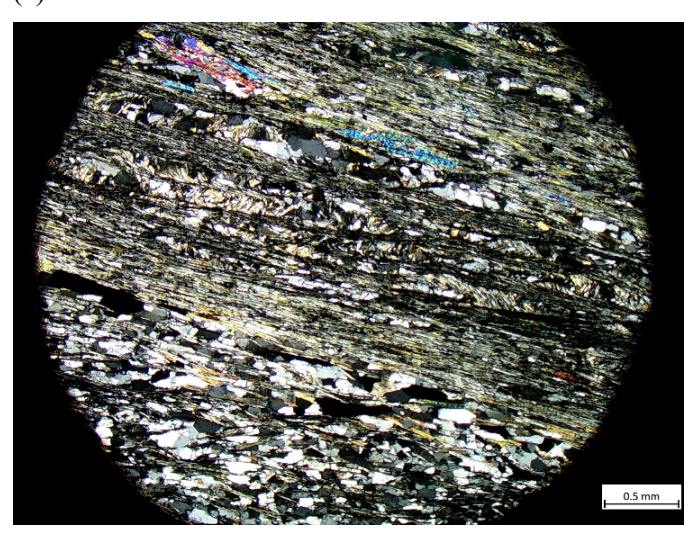
The average fracture toughness of the Poorman Schists for divider orientations is 1.68 MPa m^{1/2}, arrester is 1.25 MPa m^{1/2}, and foliation splitting is 0.77 MPa m^{1/2}. There is not abundant data on schist fracture toughness and also fracture toughness experiments comparing all three orientations in general, but our resulting fracture toughness values fall within the expected range based on previous experiments. Hu and Ghassemi (2019) also reports several values of fracture toughness measured on Poorman Schist rocks, values ranging between 1.45 and 2.22 MPa m^{1/2}. The orientation of the induced fracture relative to the foliation plane is not specified, but images of post-experiment specimens suggest that the fractures did not propagate entirely along foliation planes. Thus, results from Hu and Ghassemi (2019) do not represent foliation splitting orientation and appears to agree well with the fracture toughness values we measured in divider and arrester orientation samples.

It should be noted that in Group 3, the arrester orientation is significantly stronger than the divider orientation, contrary to the overall trend. We found that the arrester sample (7.1) shows a significantly steeper load vs. displacement slope than the divider sample (5.1) in this sample group. Poorman schist rocks are found to be more compliant when compressed normal to the foliations as shown in Figure 6 and also observed in Condon et al., 2019. Thus, we conclude that samples in Group 3 were not consistent in rock properties, thus is an invalid comparison.

We also note that Sample 10.1 of Group 4 was an outlier within the divider orientation in this group with anomalously low fracture toughness. Upon inspection of the load vs. horizontal expansion data, this sample was found to exhibit horizontal contraction whereas all other tests showed horizontal expansion as shown in Figure 7. We suspect an unexpected deformation occurred prematurely, possibly splitting along foliation, which caused this sample to expand normal to the disc face. When these invalid data are acknowledged, we find that the observation of divider fracture toughness being stronger than arrester fracture toughness is even clearer.

Finally, we also observe that Groups 2 and 5 samples exhibit larger differences in fracture toughness between different orientations indicating stronger anisotropy in fracture toughness compared to Groups 1 and 4 samples. Thin sections observations revealed that samples in group 2 and 5 exhibit stronger foliation characterized by nearlinear continuous alignment of high aspect ratio (>5) sheet silicates (Figure 9a), whereas foliation fabric in samples from Groups 1 and 4 are weaker characterized by moderate aspect ratio (<5) carbonate and quartz mineral grains. This confirms the expectation that foliation fabric strength has a significant influence on the fracture toughness of fractures propagating in different directions relative to the plane of anisotropy.

(a)



(b)



Fig. 9. Thin section images displaying (a) preferred mineral orientation and strong foliations from Group 5 Sample 12.1, and (b) weaker foliation seen in Group 1 Sample 1.1.

6. CONCLUSION

The goal of this study was to quantify the fracture toughness of the Poorman Schist at the EGS Collab Experiment 1 field site with respect to foliation orientation. We found that fracture toughness was generally highest in the divider orientation, followed by arrester, and the lowest in the foliation splitting (short transverse) orientation. Our sample groups showed a variable fracture toughness, with dividers ranging from 0.55 to 2.23 MPa·m^{1/2}, arresters ranging from 0.30 to 1.88 MPa·m^{1/2}, and foliation splitting ranging from 0.48 to 1.13 MPa·m^{1/2}. The average for each orientation was 1.68 MPa m^{1/2}, 1.25 MPa m^{1/2}, and 0.77 MPa m^{1/2}, respectively.

ACKNOWLEDGEMENTS

This material was based upon work supported by the U.S. Department of Energy, Office of Energy Efficiency and Renewable Energy (EERE), Office of Technology Development, and Geothermal Technologies Office. The research supporting this work took place in whole or in part at the Sanford Underground Research Facility in Lead, South Dakota. The assistance of the Sanford Underground Research Facility and its personnel in providing physical access and general logistical and technical support is acknowledged.

REFERENCES

- 1. Chandler, M.R., P.G. Meredith, N. Brantut, and B.R. Crawford. 2016. Fracture Toughness Anisotropy in Shale. *J. Geophys. Res. Solid Earth* 121 (3): 1706–1729 https://doi.org/10.1002/2015JB012756.
- Chang, S., C. Lee, and S. Jeon. 2002. Measurement of Rock Fracture Toughness under Modes I and II and Mixed-Mode Conditions by Using Disc-Type Specimens. *Engineering Geology* 66 (1–2): 79–97. https://doi.org/10.1016/S0013-7952(02)00033-9.
- 3. Chong, K.P., M.D. Kuruppu, and J.S. Kuszmaul. 1987. Fracture Toughness Determination of Layered Materials. *Engineering Fracture Mechanics* 28 (1): 43–54. https://doi.org/10.1016/0013-7944(87)90118-4.
- Condon, K.J., H. Sone, H.F. Wang., and The EGS Collab Team. 2019. Anisotropic Strength and Elastic Properties of Poorman Schist at the EGS Collab Experiment 1 Site. 53rd US Rock Mechanics/Geomechanics Symposium, New York, NY, USA, 23–26 June 2019, paper 19-2007.
- Fowell, R.J. 1995. Suggested Method for Determining Mode I Fracture Toughness Using Cracked Chevron Notched Brazilian Disc (CCNBD) Specimens. *Int. J. Rock Mech. and Min. Sci. & Geomech. Abstr.* 32 (1): 57–64. https://doi.org/10.1016/0148-9062(94)00015-U.
- 6. Fowell, R. J., and C. Xu. 1994. The Use of the Cracked Brazilian Disc Geometry for Rock Fracture Investigations. *Int. J. Rock Mech. and Min. Sci. & Geomech. Abstr.* 31 (6): 571–79. https://doi.org/10.1016/0148-9062(94)90001-9.
- 7. Guo, H., N. I. Aziz, and L. C. Schmidt. 1993. Rock Fracture-Toughness Determination by the Brazilian Test. *Engineering Geology* 33 (3): 177–88. https://doi.org/10.1016/0013-7952(93)90056-I.
- 8. Hu, L. and Ghassemi, A. 2019. Tensile Strength and Fracture Toughness of Poorman Schist (COLLAB). *Quarterly report to the EGS Collab Project*, 4p.
- Kneafsey, T.J., P. Dobson, D. Blankenship, J. Morris, H. Knox, P. Schwering, M. White, et al. 2018. An Overview of the EGS Collab Project: Field Validation of Coupled Process Modeling of Fracturing and Fluid Flow at the Sanford Underground Research Facility, Lead, SD. In 43rd Workshop on Geothermal Reservoir Engineering,

- Stanford University, Stanford, California, 12-14 February 2018, 1–10.
- 10. Schmidt, R.A., and C.W. Huddle. 1977. Fracture Mechanics of Oil Shale Some Preliminary Results. *Sandia Laboratory*, SAND 76-0727, https://doi.org/10.2172/7119762.